



Synthesis, crystal structure and thermal behavior of two hydrated forms of lanthanide phthalates $Ln_2(O_2C-C_6H_4-CO_2)_3(H_2O)$ ($Ln = Ce, Nd$) and $Nd_2(O_2C-C_6H_4-CO_2)_3(H_2O)_3$

David Pizon, Natacha Henry, Thierry Loiseau*, Pascal Roussel, Francis Abraham

Unité de Catalyse et Chimie du Solide (UCCS) – UMR CNRS 8181, Université de Lille Nord de France, USTL-ENSCL, Bat C7, BP 90108, 59652 Villeneuve d'Ascq, France

ARTICLE INFO

Article history:

Received 5 February 2010

Received in revised form

18 June 2010

Accepted 27 June 2010

Available online 16 July 2010

Keywords:

Lanthanides

Coordination polymer

Phthalic acid

Single-crystal XRD

2D networks

ABSTRACT

New hydrated lanthanide phthalates have been hydrothermally prepared with cerium and neodymium in different reaction media involving water or mixed water–ethanol solvent. The monohydrated $Ln_2(1,2\text{-bdc})_3(H_2O)$ ($Ln = Ce$ or Nd) and dihydrated $Nd_2(1,2\text{-bdc})_3(H_2O)_2$ forms have been characterized by single-crystal analysis. Their structures consist of infinite inorganic chains of lanthanide-centered polyhedra linked to each other through the phthalate ligands in order to generate mixed organic–inorganic layered structure. The two hydrated structures differ by the number of terminal water species attached to the lanthanide cations, which induce symmetry change from a triclinic ($Nd_2(1,2\text{-bdc})_3(H_2O)_2$) to an orthorhombic ($Nd_2(1,2\text{-bdc})_3(H_2O)_2$) cell for neodymium whereas the cerium-based phase only exists in the monohydrated form, with two distinct symmetries (orthorhombic or triclinic). Structural comparisons with the other members of the lanthanide phthalate series with identical chemical formula are also discussed. Thermal X-ray diffraction experiment indicates that the transformation from dihydrate form into the monohydrated form does not occur during a heating process.

© 2010 Elsevier Inc. All rights reserved.

1. Introduction

The research of new metal–organic framework (MOF) or polymer coordination materials has been significantly investigated for the last decade, owing to their potential applications as highly porous matrices and related properties (molecular sorption, catalysis, drug delivery, etc.) [1–10]. This class of solids mainly concerns metal carboxylates, with structures consisting of three-dimensional array of metallic nodes connected to each other through carboxyl oxygen from organic ligands. These compounds can be considered as multifunctional materials since they combine chemical properties of the organic and metallic parts. Among the different metal candidates, lanthanide cations exhibit very well-known luminescence properties and have been subject to numerous studies in this area [11,12]. For instance, the molecular assembly of such cations with N-donor or O-donor organic ligands has been intensively studied as potential luminescent probes in chemical or biological systems [13,14]. Moreover, from the crystal chemistry, the rare-earth metals have a variety of geometrical surroundings, which induce the formation of a large number of different topologies [15–19].

This contribution deals with the reactivity of phthalate anions (1,2-benzenedicarboxylate, noted 1,2-bdc) with cerium and neodymium. This specific ligand was previously reported in many compounds, which incorporate the organic linker only [20–25]. In other phases, additional complexing agents such as terephthalate [26,27], 1,10-phenanthroline [28–32] or isocotinate [33] are also used and stabilized into different atomic arrangements. The lanthanide phthalates $Ln_2(1,2\text{-bdc})_3(H_2O)$ have been isolated with the different rare-earth cations such as La [20], Eu [20], Gd [23], Tb [20], Dy [22], Tm [24], Yb [20] but the use of the lighter lanthanide metals (Ce–Nd) was not mentioned in the literature. In this paper, we report the synthesis and structure characterization of two hydrated forms of lanthanide phthalates $Ln_2(1,2\text{-bdc})_3(H_2O)$ ($Ln = Ce, Nd$) and $Nd_2(1,2\text{-bdc})_3(H_2O)_2$. They crystallize in distinct crystal symmetries, which differ from those observed in the previous compounds. The structure relationships based on the X-ray diffraction single-crystal analysis between the different forms are discussed as well as the thermal behavior of the two hydrated forms.

2. Experimental

2.1. Synthesis

The compounds have been hydrothermally prepared under autogenous pressure in a 23 ml Teflon-lined stainless steel Parr

* Corresponding author. Fax: +33 3 20 43 48 95.

E-mail address: thierry.loiseau@ensc-lille.fr (T. Loiseau).

Autoclave. The starting reactants, cerium nitrate ($\text{Ce}(\text{NO}_3)_3 \cdot 6\text{H}_2\text{O}$, Alfa Aesar, 99.5%), neodymium nitrate ($\text{Nd}(\text{NO}_3)_3 \cdot 6\text{H}_2\text{O}$, Aldrich, 99.9%) and phthalic acid ($\text{HO}_2\text{C}-\text{C}_6\text{H}_4-\text{CO}_2\text{H}$, Aldrich, 98%; noted 1,2- H_2bdc), 2,2'-bipyridyl ($\text{NC}_5\text{H}_4-\text{C}_5\text{H}_4\text{N}$, Aldrich, $\geq 99\%$) were used without any further purification. The reactions were carried out either in water or mixed water/ethanol (50/50 vol) solvent. They were placed in an autoclave and heated for 4 days at 140 °C. The resulting products were filtered off, washed with deionised water and dried at room temperature. The 2,2'-bipyridyl was originally used as additional N-donor complexing agent but was not incorporated in the final structure. However, in absence of such a molecule, no crystallized compound is obtained after the hydrothermal treatment (only re-crystallized phthalic acid is formed). This organic molecule (base) was assumed to play the role of pH regulator, which would favor the crystallization of the titled phases.

$\text{Ce}_2(1,2\text{-bdc})_3(\text{H}_2\text{O})$ (**1**): The compound **1** was synthesized from a mixture of $\text{Ce}(\text{NO}_3)_3 \cdot 6\text{H}_2\text{O}$ (208.3 mg, 0.6 mmol), 1,2- H_2bdc (199.3 mg, 1.2 mmol), 2,2'-bipyridyl (187.4 mg, 1.2 mmol) and water (10 ml, 555.6 mmol). The final pH was 2 with the production of colorless crystals.

$\text{Ce}_2(1,2\text{-bdc})_3(\text{H}_2\text{O})$ (**2**): The compound **2** was synthesized from a mixture of $\text{Ce}(\text{NO}_3)_3 \cdot 6\text{H}_2\text{O}$ (208.3 mg, 0.6 mmol), 1,2- H_2bdc (199.3 mg, 1.2 mmol), 2,2'-bipyridyl (187.4 mg, 1.2 mmol), ethanol (8 ml, 137.0 mmol) and water (8 ml, 444.4 mmol). Colorless crystals are produced at the end of the reaction.

$\text{Nd}_2(1,2\text{-bdc})_3(\text{H}_2\text{O})$ (**3**): The compound **3** was synthesized from a mixture of $\text{Nd}(\text{NO}_3)_3 \cdot 6\text{H}_2\text{O}$ (263.6 mg, 0.6 mmol), 1,2- H_2bdc (199.3 mg, 1.2 mmol), 2,2'-bipyridyl (187.4 mg, 1.2 mmol) and water (10 ml, 555.6 mmol). The final pH was 2 with the production of purple crystals.

$\text{Nd}_2(1,2\text{-bdc})_3(\text{H}_2\text{O})_2$ (**4**): The compound **4** was synthesized from a mixture of $\text{Nd}(\text{NO}_3)_3 \cdot 6\text{H}_2\text{O}$ (263.6 mg, 0.6 mmol), 1,2- H_2bdc (199.3 mg, 1.2 mmol), 2,2'-bipyridyl (187.4 mg, 1.2 mmol), ethanol (8 ml, 137.0 mmol) and water (8 ml, 444.4 mmol). Purple crystals are produced at the end of the reaction.

2.2. Single-crystal X-ray diffraction

Suitable crystals of the different samples were mounted on a glass fiber for XRD structure analysis. The crystal structure measurement was made at ambient temperature on an X8 Bruker diffractometer (Apex 2: 4K CCD detector) equipped with a graphite monochromated $\text{MoK}\alpha$ radiation with an optical fiber as collimator. For the two orthorhombic crystals (**1** and **3**) the intensities were integrated from the collected frames and corrected for background, Lorentz and polarization effects, using SaintPlus 7.53a [34] and for crystal/detector area absorption from the SADABS software [35]. Careful examination of the recorded reciprocal space of crystal **2** showed that a great number of reflections are systematically splitted and consequently, the whole recorded data could not be indexed using only one domain, suggesting the existence of a twin. Cell-Now software [36] was used to derive the two orientation matrices; it appears that the selected crystal is in fact made from two domains related by a 180° rotation about the 001 reciprocal axis, resulting in a matrix relation:

$$\begin{pmatrix} h \\ k \\ l \end{pmatrix}_{\parallel} = \begin{pmatrix} -1 & 0 & 0 \\ 0 & -1 & 0 \\ 0.6806 & 1.0515 & 1 \end{pmatrix} \begin{pmatrix} h \\ k \\ l \end{pmatrix}_I$$

Intensities were then extracted from collected frames using the program SaintPlus 7.53a [34] taking into account the two domains. After data processing, absorption corrections were performed using a semi-empirical method based on redundancy

with the TWINABS program [37]. The resulting set of “HKL4-untwined” *hkl* was used for structure resolution, while the refinements, performed with the JANA2000 software package [38], were conducted using the twinned HKLF5 set of data. Afterward refinements indicate 75.5(1)% of domain I and consequently 24.6(1)% of domain II. The same observation of systematically splitted reflections was done for crystal **4** and consequently, the same approach was tested. However, due to some broader diffraction peaks (probably resulting from a larger mosaicity of the crystal) the integration process did not converge satisfactorily. We then decided to block the integration box size at a value such that the intensities of both peaks are always integrated together and we corrected afterward from the twin effect by playing on the maximum and minimum angular difference for twin overlap, parameter that we adjusted with JANA2000 software to the value 0.9°. Using this strategy, twin ratio converged to 69.1(4)/30.9(1).

Note that for all the four studied compounds, the structures were solved primarily by direct method using SIR97 [39] and second by Fourier difference techniques. The structure refinement was performed with the JANA2000 software by the full-matrix least-squares method. A rigid-body approach of the phthalate carbon and hydrogen atoms was used to decrease the number of refined parameters and ensure a better convergence for light atoms. All refinement results are presented in Table 1. Cif files of each compound are provided as supplementary data with the online version of the article (doi:10.1016/j.jssc.2010.07.001).

2.3. Thermogravimetric analysis

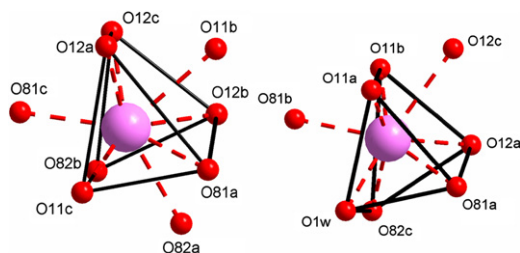
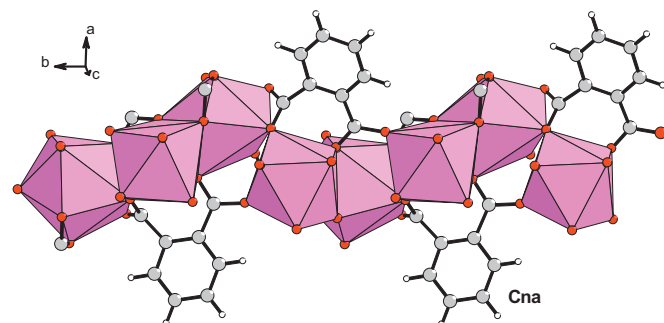
The thermogravimetric experiments have been carried out on a thermoanalyzer TGA 92 SETARAM under air atmosphere with a heating rate of 5 °C min⁻¹ from room temperature up to 1000 °C. X-ray thermodiffraction was performed under 5 l h⁻¹ air flow in an Anton Paar HTK1200N of a D8 Advance Bruker diffractometer (θ - θ mode, $\text{CuK}\alpha$ radiation) equipped with a Vantec1 linear position sensitive detector (PSD). Each powder pattern was recorded in the range 10–60° (2θ) (at intervals of 20–200 °C and at intervals of 50–750 °C) with a 0.34 s/step scan, corresponding to an approximate duration of 35 min. The temperature ramps between two patterns were 0.05 °C s⁻¹ up to 200 °C and 0.08 °C s⁻¹ from 200 °C.

3. Structure description

The structures of the compounds **1**, **2** and **3** ($\text{Ln}_2(1,2\text{-bdc})_3(\text{H}_2\text{O})$) are isotypic and built up from the connection of lanthanide cations ($\text{Ln} = \text{Ce}, \text{Nd}$) through the carboxylate groups of the phthalate ligands. In **1** and **3** (orthorhombic symmetry), there are two inequivalent crystallographic sites $\text{Ln}1$ and $\text{Ln}2$, with two distinct surroundings (Fig. 1) and three crystallographically independent phthalate species (noted “Cna”, “Cnb” and “Cnc”; *n* refers to an atom number). $\text{Ln}1$ is coordinated to nine carboxyl oxygen atoms with Ln -distances ranging from 2.406(3) to 2.759(3) Å (Ce) and 2.378(2)–2.730(1) Å (Nd) and shows a tricapped distorted trigonal prism LnO_9 polyhedron. $\text{Ln}2$ is surrounded by seven carboxyl oxygen atoms and one water oxygen atom in terminal position. It can be defined by a bicapped distorted trigonal prism $\text{LnO}_7(\text{H}_2\text{O})$. The $\text{Ln}-\text{O}$ distances are ranging from 2.374(3) to 2.759(3) Å (Ce) and 2.351(2)–2.723(2) Å (Nd). The terminal $\text{Ln}-\text{O}$ bondings are 2.516(3) (Ce) and 2.477(2) Å (Nd) and agrees with the existence of aquo species from the bond valence calculations considerations [40]. The two lanthanide $\text{Ln}1$ and $\text{Ln}2$ polyhedra share the O11b–O12a–O12c triangular face to form dimeric units $\text{Ln}1\text{Ln}2\text{O}_{13}(\text{H}_2\text{O})$ with a short $\text{Ln}1-\text{Ln}2$ distance of 4.011(1) Å (Ce) and 3.957(1) Å

Table 1
Crystal data and structure refinements for lanthanides phthalates.

	1	2	3	4
Formula	C ₂₄ H ₁₂ O ₁₃ Ce ₂	C ₄₈ H ₂₄ O ₂₆ Ce ₄	C ₂₄ H ₁₂ O ₁₃ Nd ₂	C ₄₈ H ₂₄ O ₂₆ Nd ₄
Formula weight	788.58	1577.17	796.8	1625.63
Temperature (K)	293(2)	293(2)	293(2)	293(2)
Crystal size (mm)	0.25 × 0.11 × 0.05	0.52 × 0.28 × 0.08	0.37 × 0.31 × 0.22	0.2 × 0.15 × 0.02
Crystal system	Orthorhombic	Triclinic	Orthorhombic	Triclinic
Space group	<i>Pbcn</i>	<i>P1</i>	<i>Pbcn</i>	<i>P1</i>
<i>a</i> (Å)	27.5640(4)	7.9053(2)	27.5346(3)	7.889(3)
<i>b</i> (Å)	11.4041(2)	11.7211(2)	11.3006(2)	11.570(4)
<i>c</i> (Å)	15.5519(2)	15.0873(4)	15.5119(3)	15.105(5)
α (°)	90	111.667(1)	90	111.54(2)
β (°)	90	95.073(1)	90	95.57(3)
γ (°)	90	102.134(1)	90	101.54(2)
Volume (Å ³)	4888.6(1)	1248.8(8)	4826.6(1)	1234.3(8)
<i>Z</i> , $\rho_{\text{calculated}}$ (g cm ⁻³)	8, 2.143	1, 2.097	8, 2.193	1, 2.187
μ (mm ⁻¹)	3.748	3.669	4.327	4.236
Θ range (°)	1.48–26.37	1.91–33.14	1.95–45.51	1.93–27.71
Limiting indices	–34 ≤ <i>h</i> ≤ 34 –14 ≤ <i>k</i> ≤ 14 –19 ≤ <i>l</i> ≤ 19	–12 ≤ <i>h</i> ≤ 11 –16 ≤ <i>k</i> ≤ 17 –19 ≤ <i>l</i> ≤ 23	–54 ≤ <i>h</i> ≤ 54 –22 ≤ <i>k</i> ≤ 22 –30 ≤ <i>l</i> ≤ 29	–10 ≤ <i>h</i> ≤ 10 –14 ≤ <i>k</i> ≤ 15 –19 ≤ <i>l</i> ≤ 19
Collected reflections	140,772	30,016	20,189	10,113
Unique reflections	5001	24,641	15,287	9509
Parameters	[<i>R</i> _(int) = 0.0538] 220	[<i>R</i> _(int) = 0.0434] 201	[<i>R</i> _(int) = 0.0424] 220	[<i>R</i> _(int) = 0.0568] 210
Final <i>R</i> indices	<i>R</i> ₁ = 0.0283	<i>R</i> ₁ = 0.0502	<i>R</i> ₁ = 0.0401	<i>R</i> ₁ = 0.0671
[<i>I</i> > 2σ(<i>I</i>)]	w <i>R</i> ₂ = 0.0257	w <i>R</i> ₂ = 0.0515	w <i>R</i> ₂ = 0.0380	w <i>R</i> ₂ = 0.0921
<i>R</i> indices (all data)	<i>R</i> ₁ = 0.0414	<i>R</i> ₁ = 0.0658	<i>R</i> ₁ = 0.0582	<i>R</i> ₁ = 0.0724
	w <i>R</i> ₂ = 0.0268	w <i>R</i> ₂ = 0.0528	w <i>R</i> ₂ = 0.0385	w <i>R</i> ₂ = 0.0944
Largest diff. peak and hole (e Å ⁻³)	1.11 and –1.33	2.09 and –1.39	3.42 and –3.35	6.28 and –2.16

**Fig. 1.** Lanthanide coordination polyhedron in $Ln_2(1,2\text{-}bdc)_3(\text{H}_2\text{O})$ **1** & **3**. $Ln1$ (left) is nine-fold coordinated (LnO_9) with carboxyl oxygens, with a tricapped distorted trigonal prism polyhedron. $Ln2$ (right) is eight-coordinated ($LnO_7(\text{H}_2\text{O})$) with seven carboxyl oxygens and one terminal water molecule (O1w) and shows a bicapped distorted trigonal prism polyhedron.**Fig. 2.** Representation of infinite chains of alternation of LnO_9 and $LnO_7(\text{H}_2\text{O})$ polyhedra running along the *b*-axis in $Ln_2(1,2\text{-}bdc)_3(\text{H}_2\text{O})$. The connection of the two distinct *Ln*-centered polyhedra occurs by sharing either corner or trigonal face. The connection mode of the phthalate “Cna” linker is also shown in the chain.

(Nd) further connected by sharing the O81a corner to build infinite chains $Ln_2O_{12}(\text{H}_2\text{O})$ running along the *b*-axis (Fig. 2). The four oxygen atoms also belong to the carboxylate groups of the phthalate ligand and exhibit a μ_3 connection mode. The three carboxyl oxygen atoms involved in the face-sharing are from the three different phthalates. The μ_3 -oxo corner-sharing species belong to the “Cna” phthalate. Two different situations occur for the phthalate ligands. One of the three molecules (noted “Cna”) is connected to four lanthanide cations along the inorganic chain in a bidentate bridging ($Ln1 \cdots Ln2$) mode for one carboxylate arm and both chelating ($Ln1 \cdots Ln1$) and bidentate bridging ($Ln1 \cdots Ln2$) modes for the other carboxylate arm. It adopts a $\mu_4 - \eta_1 : \eta_2 : \eta_2 : \eta_1$ configuration. The two other phthalate ligands connect two distinct chains of lanthanide polyhedra, resulting in the formation of mixed organic–inorganic layers in the (1 0 0) plane (Fig. 3). The phthalate “Cnb” is in both chelating ($Ln1 \cdots Ln1$) and bidentate bridging ($Ln1 \cdots Ln2$) modes for one carboxylate arm and the second carboxylate is in bidentate mode bridging two lanthanide cations ($Ln1$ and $Ln2$) from two distinct chains (configuration $\mu_4 - \eta_1 : \eta_2 : \eta_1 : \eta_1$). The third phthalate species “Cnc” has only tridentate and bidentate bridging fashions

($\mu_4 - \eta_2 : \eta_1 : \eta_1 : \eta_1$) and connect three adjacent lanthanide cations ($Ln1 \cdots Ln2, Ln1$) from one chain for one carboxylate group and two lanthanides ($Ln1$ and $Ln2$) from two distinct chains for the other carboxylate group. Each of the benzene ring of the three phthalate groups is pointing upward and downward the hybrid layers, along the *a*-axis. The three-dimensional cohesion of the structure is ensured by Van der Waals interaction between the aromatic rings, with the closest C–H \cdots H–C distances of around ≈ 3.04 Å (Fig. 4). The structure of the cerium phthalate also crystallizes in a triclinic cell (compound **2**) with the same atomic arrangement. Due the lower symmetry, there exist four crystallographic independent sites for the cations. Ce2 and Ce3 are eight-fold coordinated in the same manner as the $Ln2$ site in **1** and **3**, with Ce–O distances ranging from 2.389(9) to 2.655(7) Å. Ce1 and Ce4 are nine-fold coordinated (identical to $Ln1$ site in **1** and **3**), with Ce–O distance in the range 2.370(6)–2.788(7) Å.

The structure of the compound **4** ($Nd_2(1,2\text{-}bdc)_3(\text{H}_2\text{O})_2$) slightly differs from the previous one, mainly due to distinct hydration state within the coordination sphere of the lanthanide

cation. They crystallize in the low symmetry non-centric space group $P1$, resulting in four crystallographically independent sites for the trivalent metal. Two of them (Nd2 and Nd3) exhibit the same bicapped trigonal prism (Fig. 5) surrounding as Ln_2 in compounds **1**, **2** and **3**. They are eight-fold coordinated with seven carboxyl oxygens and one water molecule oxygen in terminal position, with typical Nd–O distances ranging from 2.34(3) to 2.64(4) Å. The two other cations have a different coordination since they are ten-fold coordinated with nine carboxyl oxygens and one water molecule oxygen in terminal position. The latter aquo species was not present in the previous compounds **1**, **2** and **3**. It results in a bicapped square antiprism polyhedron,

with Nd–O distances in the range of 2.32(4)–2.66(3) Å within the antiprism and slightly longer Nd–O distances (Nd–O=2.63(3)–2.84(2) Å) for the oxo and aquo species outside the square face of the antiprism. The final connection modes of the lanthanide-centered polyhedra, leading to the formation of infinite chains along the b -axis (Fig. 6) and its connection to each other in layers, are identical to the previous lanthanide phthalates **1**, **2** and **3**.

The structure of $Ln_2(1,2\text{-bdc})_3(\text{H}_2\text{O})$ is closely related to that of the series of lanthanide phthalates with the trivalent cations Eu [20], Gd [23], Tb [20] and Dy [22] adopting the same chemical formula. These compounds crystallize with a monoclinic symmetry

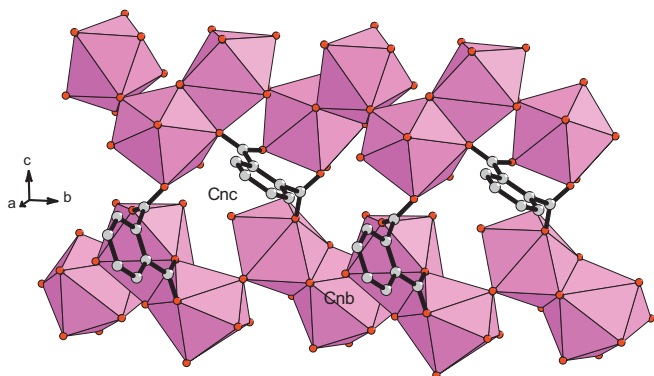


Fig. 3. View of the connection of the phthalates "Cnb" and "Cnc" with two distinct chains of lanthanide-centered polyhedra, in the (b,c) plane. Hydrogens attached to the benzene ring have been omitted for clarity.

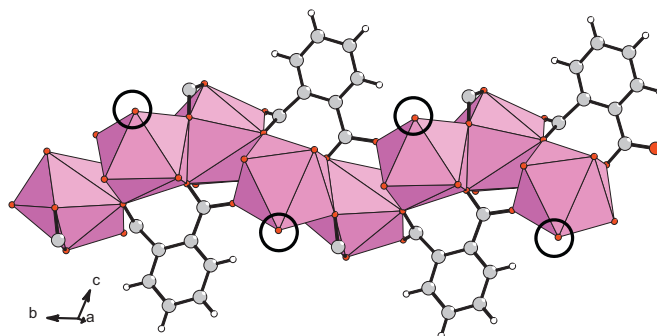


Fig. 6. View of one chain of lanthanide-centered polyhedra running along the b -axis in $\text{Nd}_2(1,2\text{-bdc})_3(\text{H}_2\text{O})_2$ (**4**). Open circles indicate the additional terminal water bounded to Nd1 and Nd4 cations.

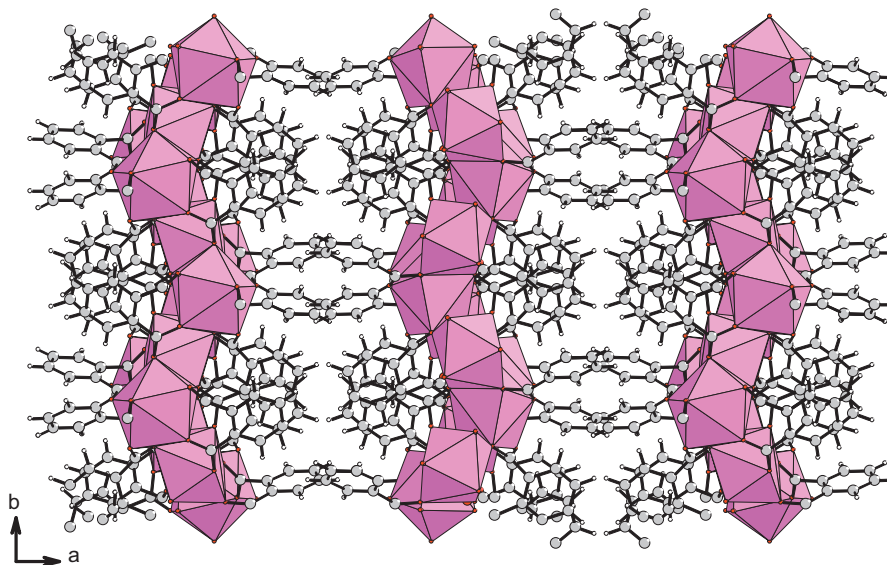


Fig. 4. View of the structure of $Ln_2(1,2\text{-bdc})_3(\text{H}_2\text{O})$ (**1** and **3**) along the c direction, showing the atomic and polyhedral arrangement of the layers of lanthanides with the phthalates groups.

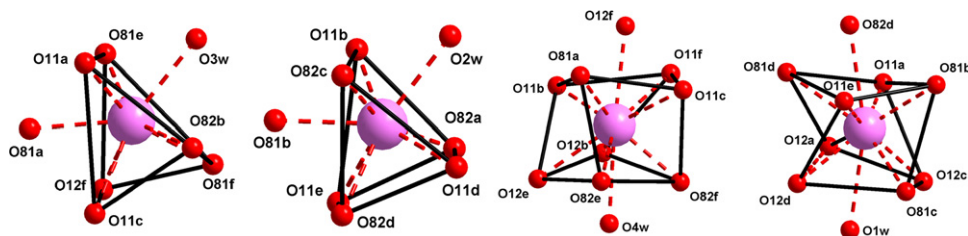


Fig. 5. Lanthanide coordination in $\text{Nd}_2(1,2\text{-bdc})_3(\text{H}_2\text{O})_2$ (**4**). From left to right, Nd2 and Nd3 are eight-fold coordinated and have a bicapped trigonal prism surrounding ($\text{NdO}_7(\text{H}_2\text{O})$). Nd1 and Nd4 are ten-fold coordinated and have bicapped square antiprism surrounding ($\text{NdO}_9(\text{H}_2\text{O})$).

($P2_1/c$) with cell parameters close to $a_M \approx 7.95 \text{ \AA}$, $b_M \approx 26.4 \text{ \AA}$, $c_M \approx 11.60 \text{ \AA}$ and $\beta \approx 107^\circ$. These values are similar to that of the compounds **1** and **3** except they are described in an orthorhombic cell ($Pbcn$) with a double a_M parameter ($2 \times 7.95 = 15.9 \text{ \AA}$ close to $a_O \approx 15.5 \text{ \AA}$, and of course β angle set to 90°). This subtle crystal change might be due to the lanthanide radius contraction, which reflects a modification of the symmetry from Ce,Nd (larger ionic radius) and the Eu–Dy (smaller ionic radius) series. With the same chemical formula, a different structure is observed for smaller lanthanides radii, such as Tm [24] or Yb [20] with the occurrence of corner-sharing infinite chains instead of face-sharing connection mode in the other compounds. At the opposite, the lanthanum-based phthalate [20] consists of double chains of metal-centered polyhedra reflecting a higher degree of condensation. Even if all the lanthanide phthalates have not been isolated, one may notice the trend of the decreasing condensation with the radius reduction with this specific ditopic ligand. However, it is unexpected that the cerium-based compound crystallizes in two symmetries with an identical chemical formula, and thus exhibits two polymorphs. From that example, it seems that the triclinic form can be obtained with different hydration states: $\text{Ce}_2(1,2\text{-bdc})_3(\text{H}_2\text{O})$ (**2**) and $\text{Nd}_2(1,2\text{-bdc})_3(\text{H}_2\text{O})_2$ (**4**).

For the two types of compounds with either the monoclinic or orthorhombic cell, the arrangement of the lanthanide-centered polyhedra connected to the phthalate is similar, but a structural distortion is observed if one considers the cationic network within an organic–inorganic layer (Fig. 7). A regular hexagonal network of lanthanide centers is clearly visible for the monoclinic compounds whereas a distorted one occurs for the other compounds **1–4**. In the orthorhombic phase (**1** and **3**), the orientation of adjacent hexagonal rings is different according to a mirror plane along the axis perpendicular to the inorganic chains, whereas the orientation of the hexagonal ring is identical in the triclinic cell (**2** and **4**).

4. Thermal behavior

The present structural study points out the isolation of two hydrated forms of lanthanide phthalates with closely related atomic arrangements and the question was if it is possible to produce the monohydrate directly from the dihydrate by heating.

A sample of $\text{Nd}_2(1,2\text{-bdc})_3(\text{H}_2\text{O})_2$ (**4**) has been characterized by thermogravimetric analysis (Fig. 8) coupled with differential thermal analysis. The curve indicates distinct weight losses occurring in several steps. The first two successive events are assigned to the departure of water molecules associated with endothermic peaks at 51 and 130 °C. It corresponds to a total observed weight loss of 6.3% at 136 °C (calculated value for $2\text{H}_2\text{O}$: 5%). The slight excess of water weight loss could be due to release of adsorbed water on the sample surface. A small weight loss of

2.4% occurred between 140 and 290 °C can be related to the beginning of decarboxylation process, already observed in the thermal decomposition of a neodymium oxalate [41]. Then, a large endothermic peak appears at 458 °C together with the weight loss of 51.1% between 290 and 750 °C. This is related to the decomposition and removal of the phthalate linker, with an expected value of 53.8%. The final product is neodymium oxide Nd_2O_3 (blue powder) with a remaining weight of 40.2% (calc. 41.2%). Before the transformation into the basic oxide, an intermediate event (5.8%) is clearly observed between 560 and 750 °C. It could be assigned to the formation of mixed oxide–carbonate of $\text{Nd}_2\text{O}_2(\text{CO}_3)$ type (calculated weight loss: 5.6%). This intermediate species was previously described during the decomposition of carboxylate lanthanides [41].

The thermal decomposition of $\text{Nd}_2(1,2\text{-bdc})_3(\text{H}_2\text{O})_2$ (**4**) was then followed by X-ray diffraction at variable temperature. The XRD patterns (Fig. 9) show no significant evolution of the Bragg peaks up to 200 °C. Detailed observation of the patterns between room temperature and 150 °C does not show any significant change, reflecting that the water removal does not modify drastically the atomic structure of the titled compound. This also indicates that the transformation of the triclinic dihydrated form into the orthorhombic monohydrated form is not observed by X-ray diffraction. This agrees with the existence of the different water content for a same symmetrical form for the compounds **2** and **4**. Then only two diffraction peaks at 7.24 ($2\theta = 6.1^\circ$) and 4.83 \AA ($2\theta = 9.2^\circ$) are visible between 250 and 350 °C, but due the lack of information, no assignment was done to this signature. Considering the previous work on the neodymium oxalate decomposition [41], it could correspond to a fully dehydrated phase, but no such a neodymium phthalate has been referenced

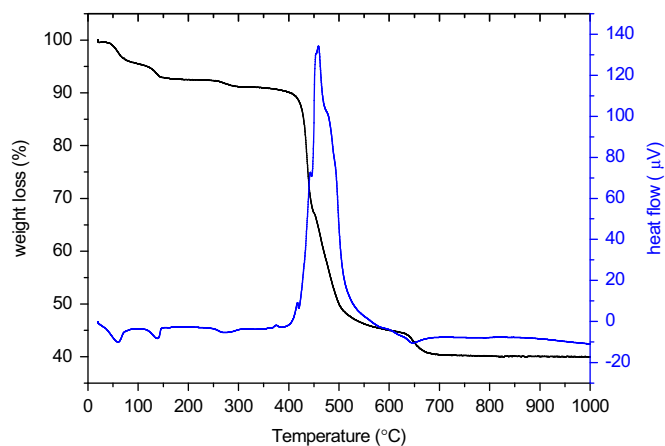


Fig. 8. TG and DT curves of $\text{Nd}_2(1,2\text{-bdc})_3(\text{H}_2\text{O})_2$ (**4**) under air atmosphere (heating rate $5 \text{ }^\circ\text{C min}^{-1}$).

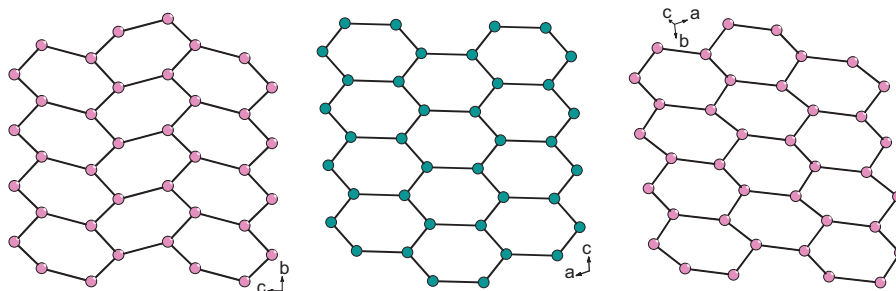


Fig. 7. Schematic views of the lanthanides cationic networks in the orthorhombic $\text{Ln}_2(1,2\text{-bdc})_3(\text{H}_2\text{O})$ (**1** and **3**) (left) monoclinic $(\text{Eu,Gd,Tb,Dy})_2(1,2\text{-bdc})_3(\text{H}_2\text{O})$ (middle) and triclinic $\text{Nd}_2(1,2\text{-bdc})_3(\text{H}_2\text{O})_2$ (**4**) phases (right).

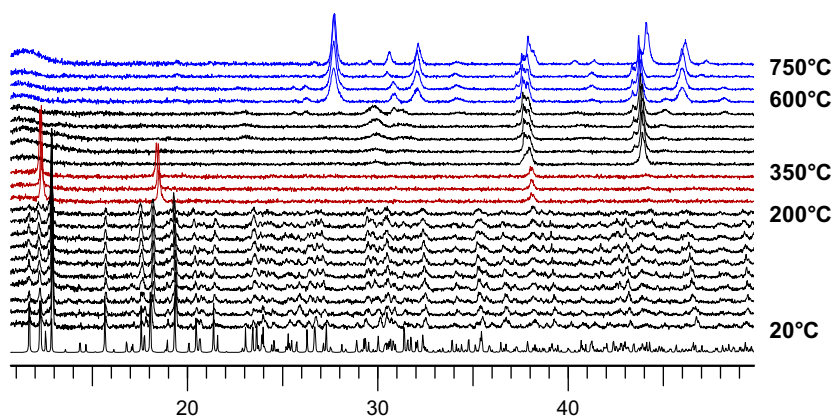


Fig. 9. X-ray thermodiffractogram of the neodymium phthalate $\text{Nd}_2(1,2\text{-bdc})_3(\text{H}_2\text{O})_2$ (**4**) (copper radiation; 20–200 every 20 °C; 200–750 every 50 °C). The first XRD pattern (bottom) corresponds to that of calculated one from the single-crystal structure. Bragg peaks appearing between 400 and 750 °C at around 38° and 44° (2θ) are assigned to those of gold used as thin film to protect the alumina sample holder.

so far. They also differ from those of the monohydrated form of neodymium phthalate. From 600 °C, the X-ray diffraction patterns indicate the crystallization of neodymium oxide (Nd_2O_3 – PDF file 74-2139).

5. Conclusion

This contribution described the hydrothermal synthesis and structural characterization of new crystalline forms of lanthanide phthalates with cerium or neodymium. Two hydrates $\text{Ln}_2(1,2\text{-bdc})_3(\text{H}_2\text{O})_x$ ($x=1,2$) exhibit structures consisting of infinite chains of lanthanide-centered polyhedra linked to each other through phthalate ligands, forming organic–inorganic layered networks. This structure type is related to that of the other lanthanide phthalates previously described with other smaller cations (Eu–Dy, Tm Yb), but crystallizing in monoclinic symmetry instead of orthorhombic one (or triclinic in case of cerium) for the titled compounds. The additional water species in the dihydrated form $\text{Nd}_2(1,2\text{-bdc})_3(\text{H}_2\text{O})_2$ is bounded to the lanthanide cation in terminal position and an increased coordination of the Nd cation is observed (ten-fold surrounding instead of nine-fold in the monohydrate). This also induces a symmetry modification since the dihydrated compounds crystallize in a triclinic form.

Acknowledgment

This work was supported by the GNR MATINEX of PACEN interdisciplinary program and by the French ANR Project no ANR-08-BLAN-0216-01.

Appendix A. Supporting information

Supplementary data associated with this article can be found in the online version at doi:10.1016/j.jssc.2010.06.021.

References

[1] O.M. Yaghi, M. O’Keeffe, N.W. Ockwig, H.K. Chae, M. Eddaoudi, J. Kim, *Nature* 423 (2003) 705.

- [2] S. Kitagawa, R. Kitaura, S.-I. Noro, *Angew. Chem. Int. Ed.* 43 (2004) 2334.
 [3] G. Férey, *Chem. Soc. Rev.* 37 (2008) 191.
 [4] A.K. Cheetham, C.N.R. Rao, R.K. Feller, *Chem. Commun.* (2006).
 [5] L. Ma, C. Abney, W. Lin, *Chem. Soc. Rev.* 38 (2009) 1248.
 [6] L.J. Murray, M. Dinca, J.R. Long, *Chem. Soc. Rev.* 38 (2009) 1294.
 [7] J.J. Perry IV, J.A. Perman, M.J. Zaworotko, *Chem. Soc. Rev.* 38 (2009) 1400.
 [8] J.Y. Lee, O.K. Farha, J. Roberts, K.A. Scheidt, S.T. Nguyen, J.T. Hupp, *Chem. Soc. Rev.* 38 (2009) 1450.
 [9] J.-R. Li, R.J. Kuppler, H.-C. Zhou, *Chem. Soc. Rev.* 38 (2009) 1477.
 [10] A.U. Czaja, N. Trukhan, U. Müller, *Chem. Soc. Rev.* 38 (2009) 1284.
 [11] K. Binnemans, *Chem. Rev.* 109 (2009) 4283.
 [12] M.D. Allendorf, C.A. Bauer, R.K. Bhakta, R.J.T. Houk, *Chem. Soc. Rev.* 38 (2009) 1203.
 [13] J.-C. Bünzli, C. Piguat, *Chem. Soc. Rev.* 34 (2005) 1048.
 [14] S.V. Eliseeva, J.-C. Bünzli, *Chem. Soc. Rev.* 39 (2010) 189.
 [15] C.L. Cahill, D.T. de Lill, M. Frisch, *CrystEngComm* 9 (2007) 15.
 [16] R.J. Hill, D.-L. Long, P. Hubberstey, M. Schröder, N.R. Champness, *J. Solid State Chem.* 178 (2005) 2414.
 [17] B.V. Harbuzaru, A. Corma, F. Rey, P. Atienzar, J.L. Jorda, H. Garcia, D. Ananias, L.D. Carlos, J. Rocha, *Angew. Chem. Int. Ed.* 47 (2008) 1080.
 [18] F.N. Shi, L. Cunha-Silva, R.A. Sa Ferreira, L. Mafra, T. Trindade, L.D. Carlos, F.A. Almeida Paz, J. Rocha, *J. Am. Chem. Soc.* 130 (2008) 150.
 [19] Y.K. Park, S.B. Choi, H. Kim, K. Kim, B.-H. Won, K. Choi, J.-S. Choi, W.-S. Ahn, N. Won, S. Kim, D.H. Jung, S.-H. Choi, G.-H. Kim, S.-S. Cha, Y.H. Jhon, J.K. Yang, J. Kim, *Ang. Chem. Int. Ed.* 46 (2007) 8230.
 [20] Y. Wan, L. Jin, K. Wang, L. Zhang, X. Zheng, S. Lu, *New J. Chem.* 26 (2002) 1590.
 [21] A. Thirumurugan, S. Natarajan, *Proc. Indian Acad. Sci.* 115 (2003) 573.
 [22] Y.-S. Song, B. Yan, Z.-X. Chen, *Can. J. Chem.* 82 (2004) 1745.
 [23] Z.-R. Meng, Q.-Z. Zhang, X.-Y. Wu, L.J. Chen, C.-Z. Lu, *Acta Crystallogr. E* 62 (2006) m1033.
 [24] G.-M. Wang, C.-S. Duan, H.-L. Liu, H. Li, *Acta Crystallogr. E* 64 (2008) m468.
 [25] S. Natarajan, A. Thirumurugan, *Inorg. Chim. Acta* 358 (2005) 4051.
 [26] A. Thirumurugan, S. Natarajan, *Inorg. Chem. Commun.* 7 (2004) 395.
 [27] A. Thirumurugan, S. Natarajan, *Eur. J. Inorg. Chem.* (2004) 762.
 [28] Y. Wan, L. Zhang, L. Jin, S. Gao, S. Lu, *Inorg. Chem.* 42 (2003) 4985.
 [29] Y.-H. Wan, L.-P. Jin, K.-Z. Wang, *J. Mol. Struct.* 649 (2003) 85.
 [30] B. Yan, Y.-S. Song, Z.-X. Chen, *J. Mol. Struct.* 694 (2004) 2004.
 [31] A. Thirumurugan, S. Natarajan, *J. Mater. Chem.* 15 (2005) 4588.
 [32] P. Li, Y. Qiu, J. Liu, Y. Ling, Y. Cai, S. Yue, *Inorg. Chem. Commun.* 10 (2007) 705.
 [33] G.-M. Wang, S.-Y. Xue, H. Li, H.-L. Liu, *Acta Crystallogr. C* 65 (2009) m469.
 [34] SAINT Plus Version 7.53a, Bruker Analytical X-ray Systems, Madison, WI, 2008.
 [35] G.M. Sheldrick, SADABS, Bruker-Siemens Area Detector Absorption and Other Correction, Version 2008/1, 2008.
 [36] G.M. Sheldrick, CELL_NOW Version 2008-2, Index Twins and Other Problem Crystals, Goettingen, Germany, 2008.
 [37] G.M. Sheldrick, Twinabs Bruker AXS Scaling for Twinned Crystals, Version 2008/1, Goettingen, Germany, 2008.
 [38] V. Petricek, M. Dusek, L. Palatinus, JANA2000, Institute of Physics, Praha, Czech Republic, 2005.
 [39] A. Altomare, G. Cascaro, G. Giacovazzo, A. Guargliardi, M.C. Burla, G. Polidori, M. Gamalli, *J. Appl. Crystallogr.* 27 (1994) 135.
 [40] N.E. Brese, M. O’Keeffe, *Acta Crystallogr. B* 47 (1991) 192.
 [41] A. Handschuh, S. Dubois, S. Vaudez, S. Grandjean, G. Leturcq, F. Abraham, *J. Nucl. Mater.* 385 (2009) 186.